Supporting Information

An *In Vitro* Model of the Gram-Negative Bacterial Cell Envelope for Investigation of Anti-Infective Permeation Kinetics

Florian Graef[1,2*], Robert Richter[1,2*], Verena Fetz[3,4], Xabier Murgia[1,2], Chiara De Rossi[1], Nicole Schneider-Daum[1], Giuseppe Allegretta[5], Walid Elgaher[5], Jörg Haupenthal[5], Martin Empting[2,5], Felix Beckmann[6], Mark Brönstrup[3], Rolf Hartmann[2,5], Sarah Gordon[1,7#] and Claus-Michael Lehr[1,2#]

[1] Department Drug Delivery, Helmholtz Institute for Pharmaceutical Research Saarland (HIPS), Helmholtz Center for Infection Research (HZI), Saarland University Campus, Building E8 1; 66123 Saarbrücken, Germany

[2] Department of Pharmacy, Saarland University, University Campus, Building E8 1, 66123 Saarbrücken, Germany

[3] Department Chemical Biology, HZI, German Center for Infection Research, Inhoffenstraße 7, 38124 Braunschweig, Germany

[4] School of Engineering and Science, Jacobs University Bremen, Campus Ring 1, 28759 Bremen, Germany

[5] Department Drug Design and Optimization, HIPS, HZI, Saarland University Campus, Building E8 1; 66123 Saarbrücken, Germany

[6] Institute of Materials Research, Helmholtz-Zentrum Geesthacht, Max-Planck-Straße 1, 21502 Geesthacht, Germany

[7] School of Pharmacy and Biomolecular Sciences, Liverpool John Moores University, James Parsons Building, Byrom Street, L3 3AF Liverpool, United Kingdom

* equally contributing

[#] Corresponding Authors: S.C.Gordon@ljmu.ac.uk; Claus-michael.lehr@helmholtz-hzi.de

Table of Contents

1.   Materials

1-hexadecanoyl-2-(9*Z*-octadecenoyl)-*sn*-glycero-3-phosphoethanolamine (POPE), 1-hexadecanoyl-2-(9*Z*-octadecenoyl)-*sn*-glycero-3-phospho-(1'-*rac*-glycerol)   (sodium salt) (POPG) and lissamine rhodamine labeled 1,2-dipalmitoyl-*sn*-glycero-3-phosphoethanolamine (Liss Rhod PE) were purchased from Avanti Polar Lipids Inc. (Alabaster, AL, USA). The PqsD inhibitor compounds 1, 2, 3, 4, 5 and 6 were synthesized in-house according to Storz *et al.*[1] The RNA polymerase (RNAP) inhibitor compounds 7, 8, and 9 were synthesized in-house according to Hinsberger *et al.*;[2] compound 10 was produced according to Elgaher *et al.*[3] Pipemidic acid was purchased from LKT Laboratories (St. Paul MN, USA), Rifampicin originated from United States Biological (Salem, MA, USA), novobiocin sodium was obtained from Cayman Chemical (Ann Arbor, MI, USA), and ciprofloxacin was obtained from Fluka® Analytical (Seelze, Germany). Tetracycline HCl was from Chemodex AG (St. Gallen, Schweiz). Transwell® permeable supports 3460 were obtained from Corning Inc. (Acton, MA, USA). Protanal LF 10/60FT (alginate) was purchased from FMC BioPolymer (Ayrshire, UK) while erythromycin, nalidixic acid, norfloxacin and smooth lipopolysaccharides (LPS; from *Escherichia coli*, 0111:B4) either with or without fluorescein isothiocyanate (FITC) label were sourced from Sigma-Aldrich (St. Louis, MO, USA). All other reagents and chemicals not specified were also obtained from Sigma-Aldrich (St. Louis, MO, USA), and were at least of analytical grade.

2.   Detailed Methods

2.1.   Structural characterization of individual models

2.1.1.   Outer membrane (OM) model

2.1.1.1. Scanning electron microscopy (SEM)

Transswell® inserts supporting inner leaflet (IL) or OM model structures were first cut out of the plastic holder surround. Vertical cross-sections of model membranes were subsequently prepared using a scalpel. Cross sections were then sputtered with gold (Quorum Q150R ES, Quorum Technologies Ltd., East Grinstead, UK) and placed in a vertical manner on sample holders before being imaged using a Zeiss EVO HD 15 scanning electron microscope (Carl Zeiss Microscopy GmbH, Jena, Germany). The thickness of IL and OM structures was then evaluated from SEM images.

2.1.1.2. Confocal laser scanning microscopy (CLSM)

CLSM was used in order to investigate the integrity of the LPS-containing OL of the OM. The IL and OM model were prepared as described in the main manuscript, employing FITC-labeled LPS to form the OL. Prepared models were imaged immediately after preparation, as well as following simulated transport experiments – this involved incubation of Transswell® inserts in Krebs-Ringer buffer (KRB; NaCl

142.03 mM, KCl 2.95 mM, K_2HPO_4 * $3H_2O$ 1.49 mM, HEPES 10.07 mM, D-Glucose 4.00 mM, $MgCl_2$ * $6H_2O$ 1.18 mM, $CaCl_2$ * $2H_2O$ 4.22 mM; pH 7.4) at 37 °C for 5 h, to allow for investigation of OL integrity following exposure to conditions to be employed in permeation studies. In preparation for imaging, Transwell® filters supporting IL or OM model structures were cut out of their plastic holder surrounds and fixed onto microscope slides using an adhesive fixing agent. Samples were then imaged using a Leica TCS SP8 AOBS/DMI8 confocal laser scanning microscope (Leica Microsystems GmbH, Wetzlar, Germany, λ_{exc}= 488 nm, λ_{em}= 545 nm), employing a 10x objective. A total of 13 regions of interest (ROI) were defined across the entire model surface, each with a surface area of approx. 3.24 mm^2. ROI were subdivided into 1800 vertical single measurements with a vertical measurement distance of 1.5 µm, so covering the overall height of each ROI. The fluorescence intensity of FITC-labeled LPS was then measured at each of these points. In addition, IL samples were prepared, imaged and analyzed in the same manner, serving as negative controls.

2.1.1.3. Correlative microscopy

As mentioned in the main manuscript, correlative microscopy was performed in order to evaluate the integrity of LPS coverage in OM models. Following sample mounting in the sample holder as described in the main manuscript, CLSM images (λ_{exc}= 488 nm, λ_{em}= 540 nm) were first acquired, followed by SEM images after sample transfer and calibration. Obtained images were then superimposed in an ultimate step using the provided software (Zeiss Zen blue 2010; Carl Zeiss Microscopy GmbH, Jena, Germany).

2.1.2. PS model

Imaging studies were carried out in order to ensure that the PS component within the overall envelope model would not be compromised by the overlying preparation of the OM model, and specifically by the use of hexane as part of OM preparation. For this purpose, the PS model was prepared as described according to the standard protocol (see main manuscript), followed by a simulated OM model deposition process − in detail, this involved two cycles of addition of 37.5 μL hexane, with oven drying at 55 °C after each addition. PS model samples exposed to hexane (and non-exposed PS model samples as negative controls) were then frozen in liquid nitrogen, and subsequently imaged via SEM (EVO HD 15; Carl Zeiss Microscopy GmbH, Jena, Germany).

2.2. Structural characterization of the overall envelope model (CLSM)

CLSM was used to investigate the three-layered structure of the overall envelope model. Each layer of the overall model was individually stained for imaging purposes. For staining of phospholipids within the IM, model preparation was carried out as previously described, with the addition of 0.1 mol% laurdan to the employed PL solution.[4] The PS model was prepared as described according to the standard protocol (see main manuscript), but on a separate Transwell® insert. The formed gel was then incubated for 1.5 h with a 500 μg/mL solution of FITC-labeled concanavalin A, known to specifically interact with alginate.[5] The FITC-labeled concanavalin A solution was

subsequently removed, and the PS model was washed twice with pre-warmed KRB to remove excess dye. The stained gel was then transferred onto the already deposited IM model. The additional transfer step was introduced to ensure that PS model staining and subsequent washing did not interfere with or alter the IM model. The OM model was added on top of the IM-PS structure as described above, with minor changes − 0.05 mol% Liss Rhod PE was added to the phospholipid mixture of the IL, and FITC-labeled LPS was employed for production of the OL. The overall envelope model was subsequently removed from the plastic support of the Transwell® holder using a scalpel, fixed on an object slide and imaged upside down on a confocal laser scanning microscope (TCS SP8 AOBS/DMI8, Leica Microsystems GmbH, Wetzlar, Germany).

2.3. Functional model characterization - transport experiments

2.3.1. OM model

For investigation of compound permeability through the OL and IL of the OM model as well as the OM model itself, transport experiments were performed. OM model-permeated amounts of fluorescent dyes (fluorescein sodium, rhodamine 123, and rhodamine B isothiocyanate) were initially tested as referred to in the main manuscript; OL and IL permeation of these dyes was also investigated. Furthermore, the permeability of vancomycin and RNAP inhibitors as anti-infective compounds across the OM model were determined. Fluorescent dyes (as detailed in Table S1), vancomycin and RNAP inhibitors were prepared in KRB (pH 7.4) at concentrations appropriate for the maintenance of sink conditions (detailed in Table S1 in the case of

fluorescent dyes; 1.18 mM in the case of vancomycin; 50 µM in the case of RNAP inhibitors). 2% of dimethylsulfoxide (DMSO) was added in the case of RNAP inhibitors in order to ensure compound solubility. Prior to transport experiments, Transwell© filter inserts supporting OL, IL or OM models were placed in cell culture plates, and pre-incubated with KRB (pH 7.4, 37 °C) for 30 min to rehydrate and equilibrate the model system. Following KRB removal, 520 µL of fluorescent dye, vancomycin or RNAP inhibitor stock solution was added to the apical compartment of each culture plate well (donor). A 1.5 mL volume of pre-warmed KRB was similarly added to the basolateral compartment (acceptor). A volume of 20 µL was then directly removed from the apical compartment, and employed to precisely measure the starting donor concentration of dye or drug. Samples of 200 µL were then taken from the basolateral compartment of each culture plate well after 0, 0.5, 1, 1.5, 2, 2.5 and in some cases additionally after 3.5 and 4.5 h, and were subsequently used to quantify the permeated amount of dye or drug as a function of time (see below, section 2.4). A final time point of 2.5 h was chosen in the case of RNAP inhibitor transport studies in order to exclude any impact of DMSO on model stability (experimentally confirmed, data not shown). Samples removed from basolateral compartments were immediately replaced with an equal volume of pre-warmed KRB, in order to maintain sink conditions throughout the course of transport experiments. Cell culture plates containing Transwell®-supported OL, IL or OM models were placed on an orbital shaker set at 150 rpm, and kept in an incubator (at 37 °C) for the duration of transport experiments.

As mentioned in the main manuscript, OM transport studies employing PMB as a well-known bacterial OM permeabilizing agent were also conducted, in order to investigate the functional similarity of the OM model to the native bacterial OM. In these studies the above mentioned fluorescent dyes were again utilized as permeability markers. In

this case, OM models in Transwell® filter inserts were pre-incubated with pre-warmed KRB for 30 min, followed by incubation for one hour with 500 µL of 1.53 mM PMB. PMB solutions were then removed, followed by washing with pre-warmed KRB; fluorescent dyes were then added to the apical compartment of culture plate wells. Samples of OM-permeated fluorescent dyes were subsequently collected from the basolateral compartment of culture plate wells at 0, 0.25, 0.5, 1, 1.5, 2 and 2.5 h. The permeated amount of fluorescent dyes at each time point was then quantified as detailed below (see section 2.4.1).

2.3.2. Overall envelope model

As referred to in the main manuscript, the general procedure for permeability investigations as described above for the OM model (section 2.3.1) was also employed in the case of the overall envelope model. The permeation behavior of fluorescent dyes (fluorescein, rhodamine 123 and rhodamine B; Table S1), was determined in this respect; the permeability of in-house synthesized PqsD inhibitors (compounds 1, 2, 3, 4, 5 and 6) and RNAP inhibitors (compounds 7, 8, 9, and 10) was also investigated. Fluorescent dye solutions were prepared in KRB pH 7.4, and applied to overall envelope models at concentrations listed in Table S1; PqsD and RNAP inhibitors were dissolved in KRB containing 2% DMSO to ensure compound solubility, and were employed at concentrations of 400 µM and 50 µM respectively to ensure sink conditions. Regarding ciprofloxacin and norfloxacin a 1 mg/mL stock solution was prepared in 0.1 M hydrochloric acid. 1 mg/mL stock solutions of pipemidic acid and nalidixic acid were prepared in 0.1 M sodium hydroxide solution. Novobiocin and tetracycline were directly dissolved in KRB to obtain a 1 mg/mL stock. Erythromycin (1

mg/mL) and rifampicin (100 µg/mL) stock solutions were prepared by dissolution in KRB containing 2% DMSO. All stock solutions were diluted to an initial donor concentration of 50 µg/mL using KRB, and the pH was adjusted to 7.4. In the case of PqsD and RNAP inhibitor transport experiments, as well as for studies employing tetracycline and nalidixic acid, samples were taken after 0, 0.5, 1, 1.5, 2 and 2.5 h. An additional time point at 4.5 h was taken in the case of erythromycin and rifampicin. In the case of the fluorescent dyes, permeation data over a 4.5 h time period are shown in the main manuscript (Figure 5). For novobiocin, ciprofloxacin, norfloxacin and pipemidic acid, samples were taken after 0, 2, 2.5 and 4.5 h.

2.4. Quantification of compound permeation

Permeated amounts of compounds in all models were always calculated according to calibration curves created from samples of standard concentrations (prepared in KRB, pH 7.4; containing 2% DMSO in the case of PqsD and RNAP inhibitors, rifampicin and erythromycin). Cumulative permeated amount in percentage was normalized to the accurately-determined start concentration in the apical (donor) compartment.

2.4.1. Fluorescence measurement

A Tecan Infinite® M200 was used to determine the permeated amount of fluorescent dyes in all studies employing these markers (see Table S1).

Table S1. Important physiochemical parameters as well as parameters for quantification of fluorescent dyes as employed in OL, IL, OM, PS and overall envelope model permeation studies.

Fluorescent dye	$\log D_{(pH\ 7.4)}$[a]	Charge at pH 7.4	Initial donor concentration (µM)	λ_{exc} (nm) – λ_{em} (nm)
Fluorescein	-0.43	-	26.6	485 – 530
Rhodamine 123	1.17	+	14.4	540 – 580
Rhodamine B	1.96	+/-	130.4	540 – 600
Rhodamine B isothiocyanate	2.03	+/-	116.6	540 – 600

[a] Values determined by the shake flask method (according to OECD guideline for the testing of chemicals section 1: physical-chemical properties, test 107).

2.4.2.   Ultra-high performance liquid chromatography (UHPLC)

A ultra-high performance liquid chromatography (UHPLC) with an Accucore™ column (RP 18, 150 mm x 2.1 mm, 2.6 µm, both from Thermo Fisher Scientific Co., Waltham, MA, USA) was used to quantify the permeated amount of vancomycin in IL and OM models in accordance with Jesus Valle et al.[6] Permeated amounts of PqsD inhibitors were quantified employing the same UHPLC and column system. A binary solvent mixture (A: water + 0.1% trifluoroacetic acid (TFA); B: acetonitrile + 0.1% TFA) was used in a gradient run, with an increase of B from an initial value of 50% to 100% in

3.7 min. A flow rate of 400 µL/min was employed, together with a column oven temperature of 30 °C. PqsD inhibitors were measured via UV detection at a wavelength of 204 nm. Retention times were 2.96 min for compound 1, 2.68 min for compound 2, 2.21 for compound 3, 1.76 min for compound 4, 1.44 min for compound 5 and 1.77 min for compound 6.

2.4.3. Liquid chromatography-mass spectrometry (LC-MS/MS)

2.4.3.1. RNAP inhibitors

A TSQ Quantum Access Max tandem quadrupole mass spectrometer coupled to an Accela UHPLC system (all from Thermo Fisher Scientific, Waltham, MA, USA) consisting of a quaternary mixing pump with a built-in solvent degassing system, thermostated autosampler, and column oven was used to quantify the permeated amount of RNAP inhibitors (Table S2). An Accucore™ RP-MS column (150 mm x 2.1mm, 2.6 µm, Thermo Fisher Scientific, Waltham, MA, USA) was also implemented, with the column oven set to 30 °C. The system was operated by the standard software Xcalibur™ (Thermo Fisher Scientific, Waltham, MA, USA). RNAP inhibitor quantification was performed using a binary solvent mixture (A: water + 0.1% formic acid; B: acetonitrile + 0.1% formic acid) and a gradient run. In the case of compounds 7, 8 and 9, B was increased from an initial value of 30% to 100% in 3 min, and kept constant for 2 min. In the case of compound 10, the percentage of B was increased from an initial value of 50% to 100% over 1 min, and kept constant for 2 min. The flow rate of the mobile phase was set to 350 µL/min, the spray voltage to 4500 mV and the capillary temperature to 330 °C in all cases. Analysis was performed operating in single reaction monitoring mode and transitions shown in Table S2 (parent mass; fragment mass) were used for identification and quantification of the compounds.

Table S2. Quantification parameters of employed RNAP inhibitors, as determined by LC-MS/MS.

Compound	Retention time (min)	Parent mass (m/z)	Fragment mass (m/z)
7	4.52	368	115.2
8	4.46	410	141.1
9	4.57	428	215.1
10	1.80	432.8	225.8

2.4.3.2. Gyrase inhibitors, novobiocin, erythromycin, rifampicin and tetracycline

While the same setup was used as for the RNAP inhibitors, the quantification parameters were altered. The temperature of the column oven was adjusted to 25 °C and the flow rate was reduced to 300 µL/min. In the case of ciprofloxacin, norfloxacin and pipemidic acid an isocratic binary solvent mixture was used with 18% of A (acetonitrile + 0.1% formic acid) and 82% of B (ammonium formate buffer 10 mM pH 3). In the case of novobiocin, tetracycline and erythromycin a gradient run was employed using the same mobile phase components, shifting from 18% to 90 % of A and from 82% to 10% of B within 2 min followed by a 3 minute hold. Due to practical reasons the quantification of erythromycin was performed by determining the main compound erythromycin A. Regarding rifampicin a gradient was used starting from 82% of A (MilliQ-water) and 18% of B (ammonium formate buffer 10 mM, pH 3) and then shifting to 10% of A and 90% of B within 3 min. The amount of A was then lowered

to 5% and B was increased to 95%. This ratio was kept for another minute. Quantification parameters can be seen below in Table S3.

Table S3. Quantification parameters of employed gyrase inhibitors, erythromycin, rifampicin, tetracycline and novobiocin, as determined by LC-MS/MS.

Compound	Retention time (min)	Spray voltage (mV)	Capillary temperature (°C)	Parent mass (m/z)	Fragment mass (m/z)
Ciprofloxacin	2.37	5500	300	332.1	231.0;245.0; 288.1;314.1
Erythromycin A	3.06	4000	280	716.3	558.4;158.0; 540.4;522.4
Nalidixic acid	3.36	5000	300	233.1	131.1;159.1; 187.1;215.1
Norfloxacin	2.28	4500	300	320.1	302.2;231.1; 276.2;282.2
Novobiocin	2.40	5000	260	613.2	189.1;133.1; 396.1;218.1
Pipemidic acid	1.69	5500	300	304.1	286.1;217.1; 215.1;189.1
Rifampicin	3.77	4500	270	823.3	791.5;399.1; 151.0;163.0
Tetracycline	2.46	4000	300	445.1	410.2;154.0; 226.0;241.0

2.5. *In bacterio* comparison − bacterial uptake studies

A 20 mL volume of lysogeny broth medium was inoculated with 0.8 mL of an *E. coli* (BW25113) overnight culture. The optical density of intact *E. coli* was then adjusted to 6 in 5 mM $MgSO_4$. Cells were subsequently incubated with 1 µM solutions (in KRB, pH 7.4) of fluorescein, rhodamine 123 or rhodamine B for 30 min. A 390 µL volume of cell suspension was then added on top of 550 µL of a 1 M sucrose cushion, and centrifuged (9 min, 4.5 *g*) to remove adherent dye. The supernatant was discarded; the cell pellet was then resuspended in 5 mM $MgSO_4$, and sonicated with a probe sonicator (Sonoplus mini 20, Bandelin electronic GmbH Co. KG, Berlin, Germany) on ice in order to disrupt the bacterial cells. A further centrifugation step was then carried out in order to sediment cell fragments (15 min, 15.7 *g*, 4 °C). The obtained supernatant was then used for quantification of internalized fluorescent dyes by LC-MS/MS.

Prior to quantification, an extraction step was carried out. A 900 µL volume of acetonitrile was added to 300 µL of internalized fluorescent dye samples, which were then vortexed and centrifuged (10 min, 15.7 *g*, 4 °C). A 1 mL volume of the resulting supernatant was then transferred to a fresh tube and dried by vacuum centrifugation (vacuum concentrator and 50 °C cold trap, Labconco, Kansas City, MO, USA) overnight to evaporate the solvent. The dried fraction was then re-dissolved in 50 µL acetonitrile (containing 0.1% formic acid and 10 ng/mL naproxen as internal standard). The solution was vortexed and centrifuged (5 min, 15.7 *g*) before transferring into vials for quantification.

A multiple reaction monitoring method was adjusted for each fluorescent compound using an AB Sciex QTrap 6500 (AB Sciex Germany GmbH, Darmstadt, Germany) coupled to an Agilent 1290 UHPLC (Agilent Technologies, Santa Clara, CA, USA).

Bacterial matrix was always included in the samples. The fluorescent dye quantification was performed using a binary solvent mixture (A: water + 0.1% formic acid; B: acetonitrile + 0.1% formic acid). A gradient run was used, where B was increased from an initial value of 1% to 10% in 1 min, followed by an increase to 100% in 3.5 min, and kept constant for 1.1 min. The flow rate of the mobile phase was set to 700 µL/min. Data was subsequently analyzed using MultiQuant software (AB Sciex Germany GmbH, Darmstadt, Germany).

3. Results and Discussion

3.1. Nebulization chamber characterization

The self-customized nebulization chamber was designed to facilitate nebulization of LPS specifically onto the filter surface of Transwell® inserts (with no contamination of the basolateral compartment or culture plate walls) in a robust and repeatable manner. As part of chamber optimization and testing, the deposition of LPS resulting from use of the self-customized chamber was analyzed employing fluorescein as a readily-quantifiable model compound. A 50 µL volume of a 10 µg/mL fluorescein solution in KRB (pH 7.4) was repeatedly nebulized via an Aerogen Solo nebulizer (Aerogen Ltd, Galway, Ireland) together with the customized chamber onto Transwell® filter inserts. Samples were subsequently taken after each nebulization step from the apical and basolateral compartment by washing with KRB and subsequently analyzed via plate reader (as described in section 2.4.1) for detection of fluorescein. Analysis revealed an appropriate and repeatable deposition of $4.56 \pm 0.17\%$ (n=9) of initially added compound in the apical compartment, and no detectable deposition in the basolateral

compartment. The developed chamber together with investigated nebulization volume of 50 µL were therefore deemed to be acceptable for LPS deposition, in order to form the OL of the OM.

3.2. IL and OM model thickness evaluation as indication for successful LPS deposition

Cross-section samples of IL and OM models were imaged and analyzed with respect to their thickness via SEM. An increase in thickness comparing IL to OM (IL+OL) model samples was taken as an initial indication of successful LPS/OL deposition on top of the phospholipid layer of the IL, and so the robustness of the described preparation procedure (Figure 2A main manuscript).
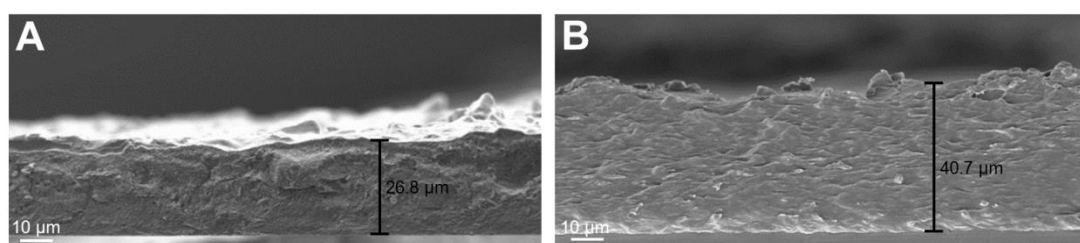

Figure S1. Vertical cross-sections of the IL (A) and overall OM model (IL+OL, B) without underlying Transwell® insert filter are shown, indicating a successful overlay of IL with OL. Images are representative of n=3 investigations, with mean z-dimension values of 28 ± 2 µm and 42 ± 5 µm for the IL and OM model samples respectively.

3.3. Integrity investigation of the OM model LPS leaflet: CLSM studies

OM model samples were analyzed via CLSM in order to investigate the distribution of the LPS layer of the OL, as well as its stability upon exposure to buffer (as would occur during transport studies). In addition, IL samples were analyzed (with and without buffer exposure) as negative controls. The definition of 13 representative ROI across the entire IL and OM model surface, within which fluorescence intensity was subsequently quantified, allowed for a more detailed analysis of the effect of permeability experiment conditions on LPS coverage (Figure S2).
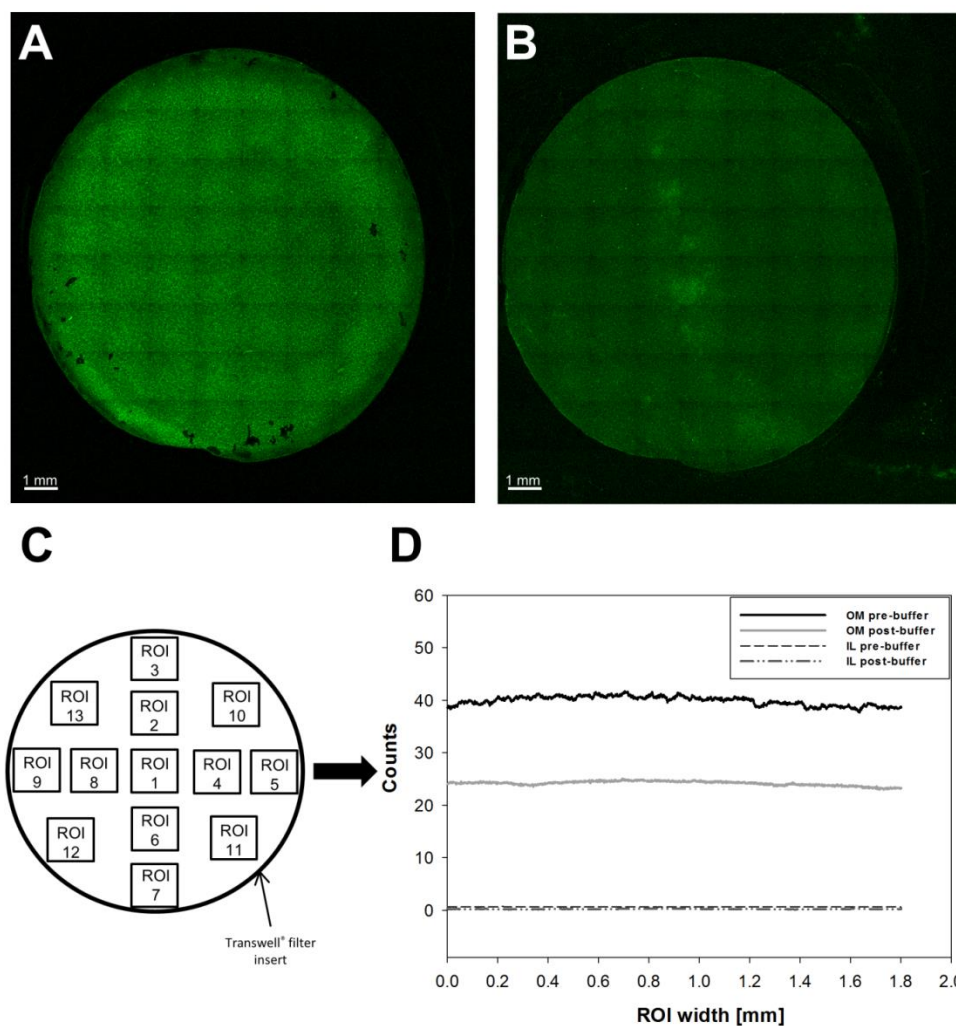
Figure S2. Representative CLSM images of the overall OM model surface showing FITC-labeled LPS in green immediately following model preparation (A), and after a simulated transport experiment involving incubation in KRB (B). The images reveal some loss of fluorescence intensity; this was further analyzed via definition of 13 representative regions of interest (ROI) on model surfaces (C), at which fluorescence intensity was quantified. Results of this quantification also indicate a drop in fluorescence intensity following a simulated transport experiment ('post buffer'), but a continued integrity of the LPS layer. The low level of fluorescence counts in the case of the IL furthermore confirms that the measured counts with respect to the OM specifically arise from FITC-labeled LPS, further providing evidence of the continued presence of appreciable amounts of LPS on buffer-exposed OM models (D).

3.4. OM model transport experiments

3.4.1. Investigation of OM model barrier properties and functional similarity

The permeability of fluorescein, rhodamine 123 and rhodamine B isothiocyanate, fluorescent dyes exhibiting a range of lipophilicities and different charges at the employed pH of 7.4, was investigated across the OL and IL alone as well as the OM (IL+OL) model (Figure S3A). Such studies were carried out in order to investigate the permeation-limiting ability of the OM, and therefore to confirm the utilization of a stable and robust OM preparation procedure. Additionally, the permeability of vancomycin, known to permeate poorly across the native OM, was investigated in the OM model in order to investigate the presence of a functional similarity (Figure S3B).
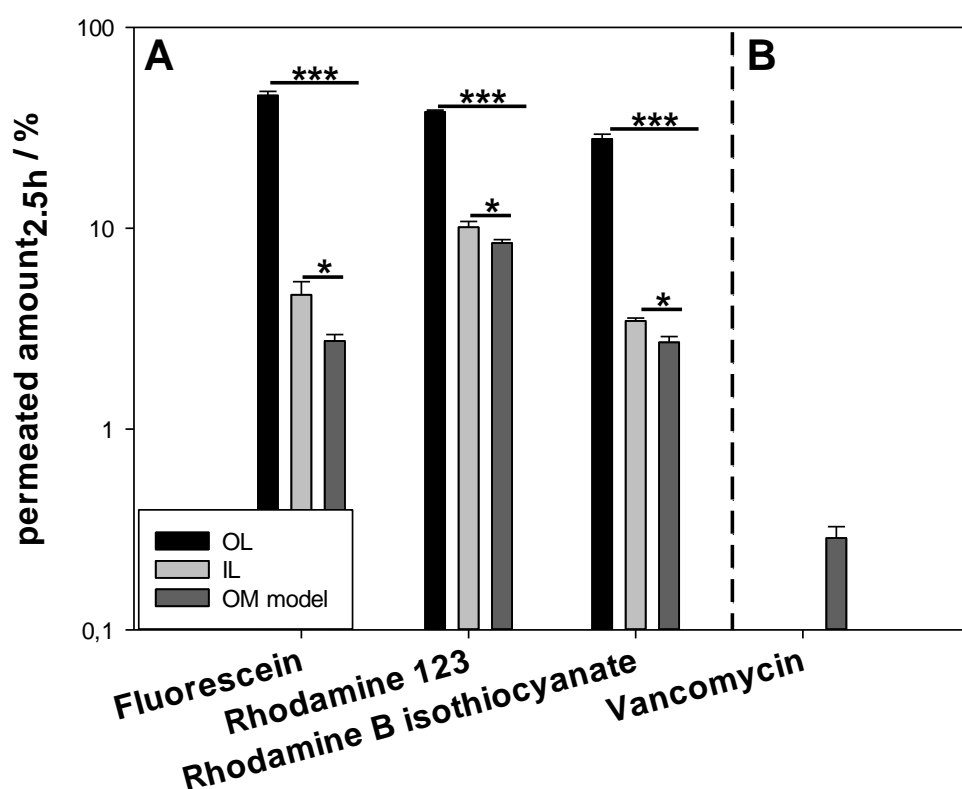
Figure S3. Permeated amounts of fluorescent dyes as permeability markers across the OL, IL and OM model are shown, revealing a significant decrease in permeated amounts in the case of the OM model in comparison to the OL or IL alone (A). This finding confirms the need to effectively combine IL and OL structures in order to form a robust and stable OM model with appreciable barrier function. Furthermore, the degree of permeation of vancomycin was shown to exhibit a very low value in comparison to tested marker dyes (B), confirming functional similarity of the OM model to the native OM. Values represent mean $\pm$ SE; n=3 for OL investigations and n=9 from 3 independent experiments for IL and OM model investigations; * = P < 0.05, *** P < 0.001.

3.4.2. PS model integrity and robustness assessment

SEM analysis of the PS model after treatment with hexane (in order to simulate OM application) as well as in its native form was carried out, in order to investigate its suitability to function as a robust spacer between the IM and OM in the overall envelope model,[7] uncompromised by overlying OM preparation (Figure S4).
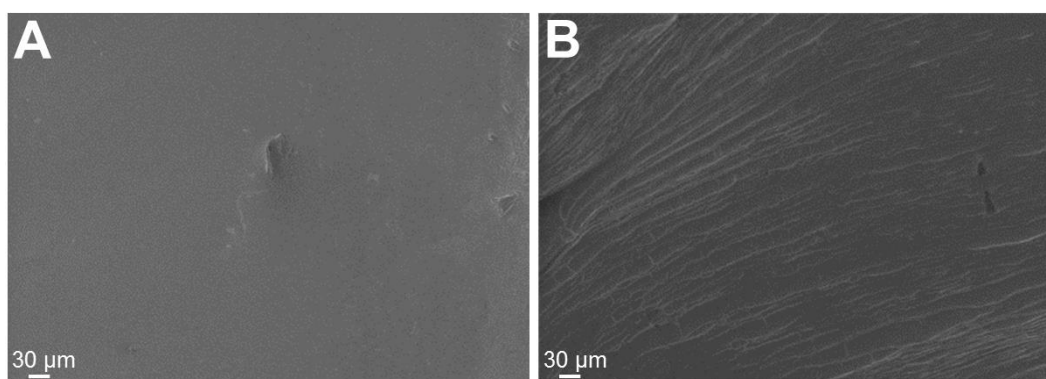

Figure S4. OM deposition on the PS model was simulated by hexane addition to assess PS model robustness in terms of the overall modeling process. PS model samples were analyzed without (A, negative control) and with hexane addition (B). SEM images reveal a slight hexane-induced change in structure but a lack of any clear structural damage, confirming continued PS model robustness.

3.4.3. Structural assessment of the overall envelope model via CLSM

As described above (see section 2.2), the overall envelope model preparation procedure was altered slightly to allow for staining of the individual components for

visualization by CLSM (Figure S5). The IM component of the overall model was stained with laurdan (blue). The PS model, which was prepared on a separate Transwell® insert, was stained with FITC-labeled concanavalin A (green), followed by transfer and placement on top of the IM. This was done to prevent any interference with or damage of the IM as a result of the PS staining and washing procedure. Liss Rhod PE (IL, red) and FITC-labeled LPS (OL, green) were employed for OM model staining.
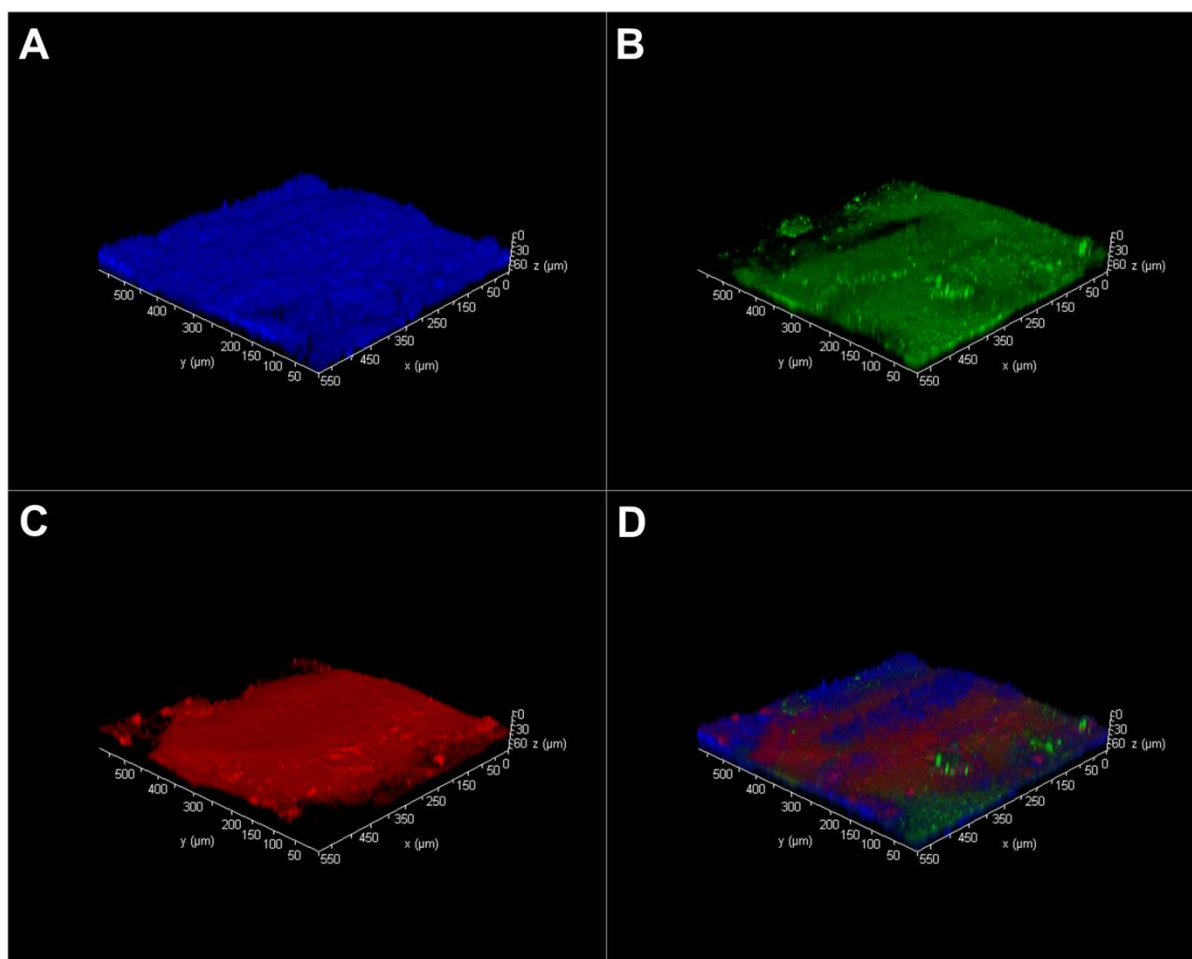

Figure S5. Z-stacks of overall model samples were performed showing individual channels of the IM model in blue (A), the PS model in green (B), the OM model in red (C) as well as the match of the channels (D). Analysis allowed for a differentiation between the 3 model components and revealed the existence of an overall model

structure composed of discrete layers, although a clear spatial differentiation of IM, PS and OM in the combined image remains difficult due to the objective-mediated limitation in resolution.

3.4.4. Overall envelope model transport experiments

Besides the permeability investigation of PqsD inhibitors (Table 1, main manuscript), a set of in-house synthesized compounds which inhibit RNAP (an enzyme responsible for transcription and essential for bacterial cell survival) was additionally selected.[8] Such compounds also need to permeate across the entire cell envelope in order to reach their target. RNAP inhibitors are known to be inactive against Gram-negative bacteria such as *E. coli* (see 'MIC in *E. coli* K12', Table S4) in many cases due to the barrier property of the OM as well as pronounced active efflux.[3] Previous minimum inhibitory concentration (MIC) assessment of the chosen compound set in *E. coli* TolC mutants, which have a non-functioning AcrAB-TolC efflux machinery, still however revealed a pair of non-active compounds (compounds 9 and 10), in addition to an active subset (compounds 7 and 8, Table S4). The permeability of this compound set in both the OM as well as the overall envelope model was therefore assessed in order to determine whether differences in passive permeability could offer an alternative explanation for observed differences in *in bacterio* activity. The initial comparison of the permeated amounts of RNAP inhibitors across the three-component overall envelope model in comparison to the one-component OM model revealed just marginal differences (Table S4), hence confirming the OM model as a major permeation barrier for this group of compounds. Furthermore the same ranking of RNAP inhibitor permeability was observed as compared to the overall model. The *E. coli* TolC-active

compounds 7 and 8 were seen to permeate through the OM as well as overall envelope model to a greater degree than the non-active compound 9, although observed differences were rather small in magnitude, potentially due to the low level of permeability in general (Table S4). Interestingly however, compound 10 was seen to exhibit the best permeability within the tested compound set, despite its inactivity in *E. coli* TolC. This effect could be explained by the low intrinsic activity of compound 10, as illustrated by its considerably higher IC_{50} value in comparison to the other tested compounds; it is also possible that the different structural backbone of compound 10 (Figure S6) may render it a substrate for efflux systems other than AcrAB-TolC. This demonstrates the ability of the envelope model to determine additional factors to permeability which influence antibiotic activity at an early stage, emphasizing the ability of the envelope model to act as an effective tool in testing novel antibiotic compounds.

Table S4. Activity in cell-free and cell-based assays as well as results of permeability investigations of employed RNAP inhibitors.
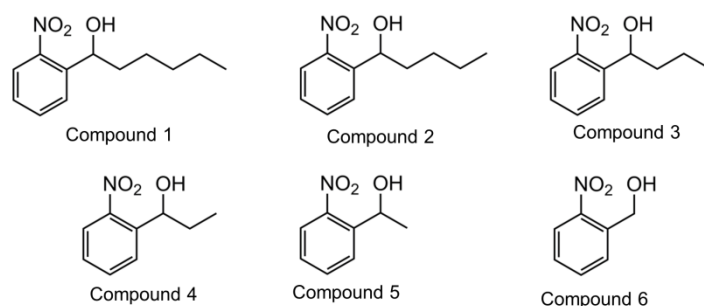
Compound	clogP	IC_{50} (µM)	MIC in *E. coli* K12[a] (µg/mL)	MIC in *E. coli* TolC[b] (µg/mL)	Permeated amounts$_{2.5 h}$ OM model[e] (%)	Permeated amounts$_{2.5 h}$ overall envelope model[e] (%)
7	7.90	13[c]	>50[c]	2.5[c]	2.28 ± 0.13	1.93 ± 0.15
8	6.95	44[c]	>25[c]	2.3[c]	2.04 ± 0.15	1.39 ± 0.14
9	7.92	13[c]	>25[c]	>25[c]	1.82 ± 0.10	1.17 ± 0.02
10	6.84	60[d]	>50[d]	>25[d]	3.42 ± 0.31	2.91 ± 0.17

[a] Minimum inhibitory concentration (MIC); *E. coli* K12: intact cell envelope system. [b] *E. coli* TolC: mutant deficient in the AcrAB-TolC efflux system. [c] Values from Hinsberger *et al.*[2] [d] Values from Elgaher *et al.*[3] [e] Values represent mean ± SE; n=6 from two independent experiments.

Structures of employed PqsD and RNAP inhibitors

PqsD inhibitors

Compound 1   Compound 2   Compound 3

Compound 4   Compound 5   Compound 6

RNAP inhibitors

Compound 7   Compound 8

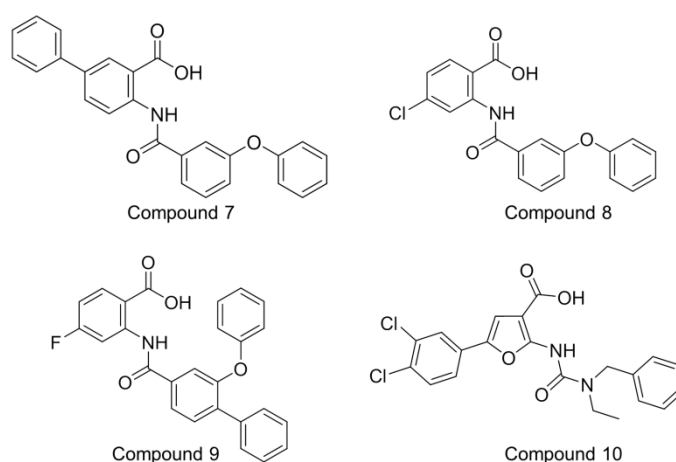Compound 9   Compound 10

Figure S6. Overview of structures of employed PqsD and RNAP inhibitors.

4.   References

1. Storz, M. P., Allegretta, G., Kirsch, B., Empting, M., and Hartmann, R. W. (2014) From in vitro to in cellulo: structure-activity relationship of (2-nitrophenyl)methanol derivatives as inhibitors of PqsD in Pseudomonas aeruginosa. *Org. Biomol. Chem. 12*, 6094-6104. DOI:10.1039/c4ob00707g.

2. Hinsberger, S., Husecken, K., Groh, M., Negri, M., Haupenthal, J., and Hartmann, R. W. (2013) Discovery of novel bacterial RNA polymerase inhibitors: pharmacophore-based virtual screening and hit optimization. *J. Med. Chem. 56*, 8332-8338. DOI:10.1021/jm400485e.

3. Elgaher, W. A. M., Fruth, M., Groh, M., Haupenthal, J., and Hartmann, R. W. (2014) Expanding the scaffold for bacterial RNA polymerase inhibitors: design, synthesis and structure-activity relationships of ureido-heterocyclic-carboxylic acids. *RSC Adv. 4*, 2177-2194. DOI:10.1039/C3RA45820B.

4. Graef, F., Vukosavljevic, B., Michel, J. P., Wirth, M., Ries, O., De Rossi, C., Windbergs, M., Rosilio, V., Ducho, C., Gordon, S., and Lehr, C. M. (2016) The bacterial cell envelope as delimiter of anti-infective bioavailability - An in vitro permeation model

of the Gram-negative bacterial inner membrane. *J. Control. Release 243*, 214-224. DOI:10.1016/j.jconrel.2016.10.018.

5. Strathmann, M., Wingender, J., and Flemming, H. C. (2002) Application of fluorescently labelled lectins for the visualization and biochemical characterization of polysaccharides in biofilms of Pseudomonas aeruginosa. *J. Microbiol. Methods. 50*, 237-248.

6. Jesus Valle, M. J., Lopez, F. G., and Navarro, A. S. (2008) Development and validation of an HPLC method for vancomycin and its application to a pharmacokinetic study. *J. Pharm. Biomed. Anal. 48*, 835-839. DOI:10.1016/j.jpba.2008.05.040.

7. Zgurskaya, H. I., Löpez, C. A., and Gnanakaran, S. (2015) Permeability barrier of Gram-negative cell envelopes and approaches to bypass it. *ACS Infect. Dis. 1*, 512-522. DOI:10.1021/acsinfecdis.5b00097.

8. Chopra, I. (2007) Bacterial RNA polymerase: a promising target for the discovery of new antimicrobial agents. *Curr. Opin. Investig. Drugs. 8*, 600-607.